ChemComm

COMMUNICATION

View Article Online
View Journal | View Issue

Cite this: *Chem. Commun.*, 2019, 55, 12980

Received 11th August 2019,
Accepted 2nd October 2019

DOI: 10.1039/c9cc06210f

rsc.li/chemcomm

An ultrasensitive electrochemiluminescence biosensor for nuclear factor kappa B p50 based on the proximity hybridization-induced hybridization chain reaction†

Xiaocui Huang,[a] Ying Zhang,[a] Wen Xu,[b] Wei Xu,*[b] Longhua Guo,[a] Bin Qiu[a] and Zhenyu Lin*[a]

Nuclear factor kappa B p50 (NF-κB p50) induces various biological processes. In this study, a highly selective and sensitive electrochemiluminescence (ECL) biosensor for the detection of NF-κB p50 has been developed, which combines the high selectivity of the proximity hybridization assay (PHA) with the high efficiency of the hybridization chain reaction (HCR).

Nuclear factor kappa B p50 (NF-κB p50) is a sequence-specific DNA-binding protein (with specific binding sequences of 5′-GGAAAGTCCC-3′ and 3′-GGGACTTTCC-5′,[1] marked in yellow in Scheme 1) that acts as an important transcription factor in cells and is involved in the response of cells to external stimuli. Studies have confirmed that incorrect regulation of NF-κB p50 in cells is associated with a variety of diseases.[2] Therefore, the highly sensitive and specific detection of NF-κB p50 is of great significance. To date, many analytical methods for the selective quantification of DNA binding proteins had been developed, such as electrophoretic mobility shift assay (EMSA),[3] enzyme-linked immunosorbent assay (ELISA),[4] and western blotting. Recently, biosensors based on fluorescence and electrochemistry detection technologies had been proposed for NF-κB p50 detection.[5]

Electrochemiluminescence (ECL) is the process in which electrogenerated radicals undergo electron-transfer reactions to form excited species emitting light.[6] It was first described by Profs. Hercules and Bard in the mid-1960s,[7] and has become a powerful analytical technology in many fields.[8] To the best of our knowledge, ECL bioassay for NF-κB p50 detection has not been reported yet. $Ru(phen)_3^{2+}$ is a highly efficient ECL luminescent reagent and can be inserted into the dsDNA groove.[9] These characteristics had been applied to develop many sensitive ECL biosensors.[10] But in most of these biosensors, DNA stack assembly on the electrode was usually achieved by growing long strands of dsDNA on the surface of the electrodes directly. Which has the disadvantages such as time consuming and low assembly efficiency due to steric hindrance. Earlier, our group developed homogeneous ECL biosensors, which have the advantage of simple operation and effectively reduce the steric hindrance effect.[11] But this technique needs the utilization of ultrafiltration to reduce the interfering signals from $Ru(phen)_3^{2+}$ which had not been interacted with the dsDNA; the process is cumbersome, time consuming, and its low separation efficiency may lead to high background signals. It is still necessary to develop new strategies to solve the above problems.

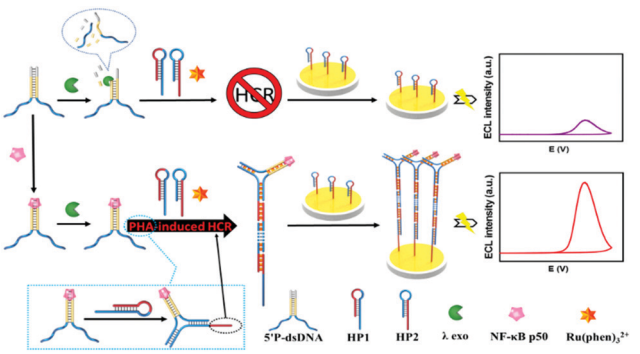

Scheme 1 The principle of the proposed ECL biosensor for NF-κB p50.

Hybridization chain reaction (HCR) is an enzyme-free isothermal nucleic acid signal amplification technology, which does not require strict reaction conditions, the products of which are long dsDNAs.[12] Proximity hybridization assay (PHA), as a DNA-assisted protein assay technology, is gaining more and more attention in clinical diagnosis.[13] The technique shows high specificity by specific binding of a single target protein to two probes. And the conversion of protein analysis to DNA detection also gives it an advantage to improving the sensitivity. The excellent characteristics of PHA in sensing applications provide more new ideas for the design of sensing systems.

[a] *Ministry of Education Key Laboratory for Analytical Science of Food Safety and Biology, Fujian Provincial Key Laboratory of Analysis and Detection for Food Safety, College of Chemistry, Fuzhou University, Fuzhou, Fujian, 350116, China. E-mail: zylin@fzu.edu.cn; Fax: +86-591-22866135; Tel: +86-591-22866135*

[b] *Department of Pharmacy, Fujian University of Traditional Chinese Medicine, Fuzhou, Fujian, 350122, China. E-mail: 2000017@fitcm.edu.cn*

† Electronic supplementary information (ESI) available: Materials and instruments and the results about the application of the proposed method. See DOI: 10.1039/c9cc06210f

In this study, an ECL biosensor that combines PHA and HCR for highly specific, ultrasensitive detection of NF-κB p50 has been developed. The principle of the HCR-based ECL sensor for quantitative detection of NF-κB p50 is shown in Scheme 1. Two well-designed ssDNAs (5′P-DNA1 and DNA2) can hybridize to form a partially complementary proximity complex (5′P-dsDNA) containing a specific binding site for the NF-κB p50 protein and two single-stranded branch segments (shown in blue). When NF-κB p50 is present, NF-κB p50 binds to 5′P-dsDNA, protecting 5′P-dsDNA from cleavage by lambda exonuclease (λ exo). The delicately-designed HCR material hairpin DNAs (HP1 and HP2) complement each other, but kinetically hindered due to their complementary regions being locked in the hairpin stem. The two single-stranded fragments of the protected 5′P-dsDNA are adjacent to each other and can act synergistically as a trigger to open the stem part of HP1 by a toehold-mediated strand displacement reaction. The newly exposed single-stranded DNA region within HP1 can hybridize to HP2 *via* secondary toehold-mediated DNA strand displacement. The newly exposed single-stranded DNA region of the opened HP2 can also act as a trigger to induce another hairpin HP1 to open, thereby catalyzing the hybridization of HP1 and HP2 until HP1 or HP2 is exhausted. At the same time, plenty of $Ru(phen)_3^{2+}$ as ECL molecular beacons was embedded in the dsDNA double helix regions and act as an ECL indicator. Since the hairpin HP2 added to the system is relatively excessive than HP1, the HCR amplification products are long dsDNAs with HP2 as the bulging end (5′P-dsDNA-(HP1–HP2)$_n$). The HP2 protruding end (marked in blue) of 5′P-dsDNA-(HP1–HP2)$_n$ can hybridize with the capture hairpin probe (HP1-SH) that was modified on the gold electrode surface, opening HP1-SH and capturing the HCR product onto the electrode, so an enhanced ECL signal can be detected. Conversely, if NF-κB p50 is absent, the 5′P-dsDNA will be digested by λ exo and the two single-stranded fragments are not adjacent in solution, so HP1 cannot be opened and HCR cannot be activated. In this case, very little amount of $Ru(phen)_3^{2+}$ can be embedded in the HP1-SH stem modified on the surface of the electrode, so that only a low ECL signal can be detected. The ECL intensity detected had a relationship with the amount of NF-κB p50, and a sensitive method for NF-κB p50 detection can be developed.

Polyacrylamide gel electrophoresis, electrochemical impedance spectroscopy (EIS) and ECL were used to verify the feasibility of the proposed strategy. The products of each step were analyzed by polyacrylamide gel electrophoresis (as shown in Fig. 1A) firstly. The lanes a and b showed that 5′P-dsDNA was digested by λ exo in the absence of NF-κB p50, and when NF-κB p50 was present, the 5′P-dsDNA was protected from enzymatic cleavage. The lanes c, d, and e indicated that HCR amplification would not occur when no trigger was added (lane c) or 5′P-dsDNA was digested by using λ exo without target protection (lane d). The HCR amplification can only be induced by the presence of target-protected 5′P-dsDNA (lane e). In addition, the feasibility of the opening of HP1 induced by PHA is shown in Fig. S1 in the ESI.†

Fig. 1B shows the change in impedance at different modification stages. Compared with the bare gold electrode (curve a), the impedance of the gold electrode modified with HP1-SH was significantly increased due to the electrostatic repulsion between

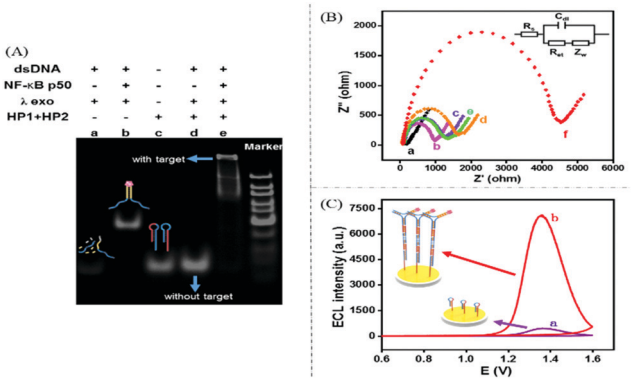

Fig. 1 Feasibility of the ECL biosensor. (A) Polyacrylamide gel electrophoresis analysis under different conditions. (B) Electrochemical impedance spectroscopy of various probes modified at electrode: (a) bare Au electrode, (b) electrode 'a' + HP1-SH, (c) electrode 'b' + MCH, (d) electrode 'c' + NF-κB p50, (e) electrode 'c' + 5′P-dsDNA + λ exo + HP1 + HP2, (f) electrode 'c' + 5′P-dsDNA + NF-κB p50 + λ exo + HP1 + HP2 in 5.0 mM $[Fe(CN)_6]^{3-/4-}$ including 100 mM KCl. (C) ECL intensity of the proposed sensing system in the (a) absence and (b) presence of 10 nM NF-κB p50.

the negatively charged hairpin probes HP1-SH and $[Fe(CN)_6]^{3-/4-}$ (curve b). A further increase in impedance could be observed when the unmodified site of the electrode surface was blocked by MCH (curve c). The electrode "c" was immersed in 10 nM κB p50 in the experiment as a negative control (curve d). Curve d showed a small increase in impedance compared to curve c, which indicated that the target protein has less non-specific adsorption on the MCH-blocked electrode. In the absence of the initiator, HP1-SH existed in the form of a stable hairpin structure that could not capture the introduced HP1 and HP2, so the impedance did not increase significantly (curve e). After the target binding-induced HCR amplification reaction, HP1-SH modified on the electrode surface captured the HCR product (curve f). The impedance of curve f was significantly larger than that of curve d and curve e, which indicated that the increase in impedance of the positive control is mainly due to the accumulation of the HCR product on the electrode surface, instead of the target protein. These results also indicated that the proposed biosensor was successfully prepared. The ECL character of the system had also been studied. In the absence of the target, only a very small amount of $Ru(phen)_3^{2+}$ was inserted into the double-stranded portion of the hairpin HP1-SH stem, so only a weak ECL signal was detected (curve a in Fig. 1C), whereas in the presence of 10 nM NF-κB p50, a large amount of $Ru(phen)_3^{2+}$ was inserted into the amplified product dsDNA, and the ECL signal was significantly enhanced (curve b in Fig. 1C). All the above results confirm the feasibility of the proposed sensor.

In order to obtain the best sensing performance, the effects of several important experimental parameters have been optimized. In this detection system, the binding time between NF-κB p50 and the specific sequence was directly related to the sensing effect of the target. As shown in Fig. 2A, as the binding time increases, ΔECL (ΔECL = ECL − ECL_0, ECL and ECL_0 are the ECL intensity in the presence and absence of NF-κB p50) intensity enhanced first

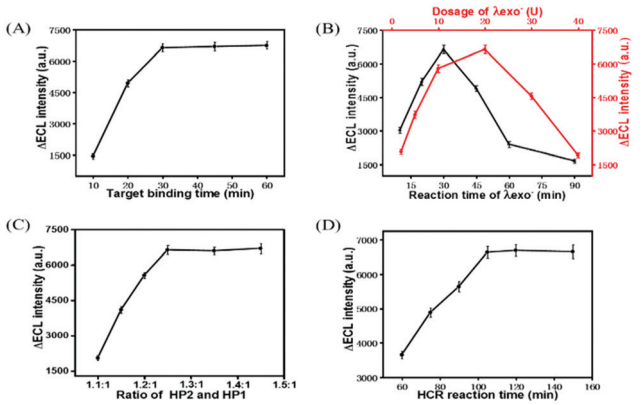

Fig. 2 Optimization of the detection conditions: (A) the binding time between NF-κB p50 and 5′P-dsDNA. (B) Dosage of λ exo (with a digestion time of 30 min) and the digestion time of λ exo (with 20 U λ exo). (C) The ratio of HP1 and HP2. (D) The HCR reaction time (also the intercalating time of $Ru(phen)_3^{2+}$ into dsDNA grooves). All the detections were performed in 6.7 mM phosphate buffer (pH 7.4) containing 20 mM TPA. Scan range: 0.2 to 1.6 V. Scan rate: 50 mV s^{-1}. The NF-κB p50 concentration was 10 nM.

and reached a plateau after 30 min, indicating that 30 min was sufficient for NF-κBp50 binding. Therefore, 30 min was chosen as the optimal binding time for NF-κB p50 and its adapted dsDNA.

An insufficient enzyme amount or cleavage time will result in a large background signal, while too much enzyme or a long cleavage time will result in non-specific digestion of 5′P-dsDNA and failure to open HP1. The HCR reaction will not be triggered, generating a false experimental signal. Thus, it is necessary to optimize the dosage of λ exo and the cleavage time in the experiment. As shown in Fig. 2B, ΔECL increased with an increase of the λ exo dosage and the digestion time first and then reduced. At an enzyme dosage of 20 U and a cleavage time of 30 min, ΔECL reached its maximum, respectively, after which ΔECL decreased due to the influence of λ exo on the non-specific cleavage of the two single-stranded fragments of 5′P-dsDNA. Therefore, 20 U λ exo and 30 min digestion times were selected for subsequent experiments.

HCR amplification products are long dsDNAs, and the material hairpin HP2 added should be in excess of HP1 to ensure that the products end with HP2. So the ratio of HP2 to HP1 was optimized in the experiment. As shown in Fig. 2C, when HP2 : HP1 was 1.25 : 1, ΔECL reached the platform, indicating that the ratio of HP2 to HP1 is 1.25 : 1 was sufficient to ensure that the HCR reaction time was 105 min, one of the material hairpin of HCR was depleted, a sufficient amount of $Ru(phen)_3^{2+}$ was embedded in the dsDNA grooves, ΔECL reached the plateau, indicating that the reaction was completed at this time. So 105 min was chosen as the optimal HCR time in the following study. The sensitivity and linear range of the biosensor were explored under optimized conditions. As shown in Fig. 3A, the ECL intensity of the system increased with the increasing NF-κB p50 concentration. The ΔECL intensity increased with the increasing target concentration and showed a good linear relationship with the logarithm of the NF-κB p50 concentration in the range of 0.5 pM–300 nM, (Fig. 3B). The regression equation was:

$$\Delta ECL = 1498.98 \lg C/\mathrm{nM} + 5321.43 \quad R^2 = 0.994$$

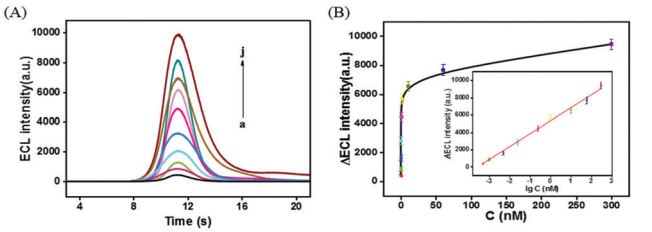

Fig. 3 (A) ECL spectra at different concentrations of NF-κB p50. a–j: 0, 0.5 pM, 1 pM, 5 pM, 25 pM, 250 pM, 1 nM, 10 nM, 60 nM, and 300 nM. (B) The relationship between ECL and the logarithm of NF-κB p50 concentrations. All the detections were performed in 6.7 mM phosphate buffer (pH 7.4) containing 20 mM TPA. Scan range: 0.2 to 1.6 V. Scan rate: 50 mV s^{-1}.

where C was the NF-κB p50 concentration and R^2 was the correlation coefficient. The detection limit was 0.2 pM (S/N = 3).

In order to further explore the superiority of the proposed biosensor, the ECL response between the method of gradually growing long chain-like dsDNA on the electrode surface (the on-surface-HCR-based method, Scheme S2 in the ESI†) and the method of assembling long chain-like dsDNA into the electrode in this strategy was compared. As shown in Fig. S2A (ESI†), compared to the method of inducing HCR amplification on the electrode surface and gradually growing long chain-like dsDNA, a much larger ECL signal was obtained by using the method of assembling the HCR product 5′P-dsDNA-$(HP1–HP2)_n$ to the electrode surface after HCR amplification in a homogeneous solution. The reason may be that the on-surface-HCR-based method requires the protein to be close to the electrode surface during probe hybridization. The probe hybridization rate may be low due to the low protein capture rate. And the accumulation of proteins on the electrode surface may affect the electron transfer process on the electrode surface and eventually lead to a small ECL signal. The method proposed by this strategy can prevent the protein from accumulating on the surface of the electrode, and maximize the ECL signal output of $Ru(phen)_3^{2+}$ embedded in dsDNA. In addition, compared with the on-surface-HCR-based method, the homogeneous HCR reaction system in this work is more favorable for high-efficiency amplification. Moreover, not all processes are performed on the surface of the electrode, which can shorten the detection time by 2.5 h.

Compared to other methods reported, the proposed ECL biosensor has a lower detection limit and a wider linear range (refer to Table S1 in the ESI†). This higher sensitivity and the wider detection range can be attributed to the high sensitivity of the ECL detection technique, the high amplification efficiency of HCR, and the accumulation of the electrochemiluminescent active compound $Ru(phen)_3^{2+}$ on the gold electrode surface *via* electrostatic interaction.

The selectivity of our strategy was investigated by assessing the degree of non-specific binding of interfering proteins to dsDNA. Four possible interfering proteins were studied under the same experimental conditions, including GP73, BSA, AFP and CEA. As shown in Fig. S2B in the ESI,† when the proposed sensors were used to detect GP73 (10 nM), BSA (10 nM), AFP (10 nM) and CEA (10 nM), the ECL response was almost indistinguishable from the blank test. The ECL intensity of

the mixed samples of the above four interfering substances (10 nM) and NF-κB p50 (100 pM) was comparable to that of NF-κB p50 (100 pM), and the ECL intensity was significantly enhanced. These experimental results indicate that our strategy is highly selective for NF-κB p50 detection.

To further evaluate the application of the proposed strategy for real biological samples, HeLa cell lysates were used as real samples to study the feasibility of the sensor in actual biological sample detection by detecting the concentration of NF-κB p50 in the cell lysates and calculating the recovery of the spiked sample. The results are shown in Table S2 in the ESI.† The lysates of 6000 cells were directly measured in the experiment at a p50 concentration of 0.95 pM. HeLa cell lysates were spiked with NF-κB p50 at five concentrations, and the recovery was 96.8–104.1% with a relative standard deviation of 2.87–5.74%. These results indicated that our strategy has the ability to detect actual samples and is expected to be used in clinical assays.

Inhibition of overexpression of transcription factors is an important goal of drug development. Oridonin is a known NF-κB p50 inhibitor that inhibits the binding between NF-κB p50 and its recognition component. In this study, oridonin was incubated with NF-κB p50 to investigate the inhibitory effect of oridonin. As shown in Fig. S3 in the ESI,† in the absence of an inhibitor, NF-κB p50 can efficiently bind 5′P-dsDNA and protect 5′P-dsDNA from enzymatic digestion, thus obtaining a high ECL signal. Since oridonin inhibits the binding between NF-κB p50 and 5′P-dsDNA, the relative intensity measured gradually decreases as the concentration of oridonin increases, compared to the ECL intensity when no oridonin is added. In addition, it was also observed that 1 μM of oridonin could substantially inhibit the NF-κB activity of 500 pM. These results demonstrate the ability of the proposed strategy to screen and quantify the relevant inhibitors of NF-κB p50, as well as the potential to assess the NF-κB p50-targeted drugs.

In summary, a simple, ultrasensitive and highly selective ECL biosensor for NF-κB p50 detection had been developed. The biosensor utilizes $Ru(phen)_3^{2+}$ as an ECL beacon to output the signal, and the target binding protection induces HCR amplification to amplify the signal. The greatest feature of the proposed sensor lies in that the HCR reaction occurs in a homogeneous solution first and is captured by a probe first immobilized on the electrode surface. Compared to the earlier reported methods requiring HCR to occur at the interface between the electrode surface and the solution, the proposed method reduced the detection time, and reduced the steric hindrance effect by avoiding enrichment of the protein on the electrode surface. Compared to the reported related literature, the biosensor operates more simply, with lower detection limits and a wider linear range. The biosensor has been successfully applied to the detection of NF-κBp50 in cell lysates with satisfactory results. Studies of the inhibition of this protein also indicate that the proposed strategy has the ability to screen and quantify the related inhibitors of NF-κBp50. Based on the excellent analytical performance of NF-κB p50, the proposed method has certain potential application value for the diagnosis of NF-κB p50-related diseases and the evaluation of NF-κB p50 targeted drugs. Furthermore, by changing the aptamer binding sequence, this strategy is also expected to be applied to the detection of other biomarkers.

This project was financially supported by the National Natural Science Foundation of China (21775026, 21575025, and 21575027), the Program for Changjiang Scholars and Innovative Research Team in University (No. IRT15R11), the cooperative project of production and study in University of Fujian Province (2018Y4007), the Science Foundation of Fujian Province (2018J01685 and 2018J01682), and the STS Key Project of Fujian Province (2017T3007).

Conflicts of interest

There are no conflicts to declare.

Notes and references

1 F. E. Chen, D.-B. Huang, Y.-Q. Chen and G. Ghosh, *Nature*, 1998, **391**, 410–413.
2 (*a*) J. Caamano and C. A. Hunter, *Clin. Microbiol. Rev.*, 2002, **15**, 414–429; (*b*) G. E. Griffin, K. Leung, T. M. Folks, S. Kunkel and G. J. Nabel, *Nature*, 1989, **339**, 70–73; (*c*) L. Lu, H. Su and F. Li, *Anal. Chem.*, 2017, **89**, 8328–8334.
3 J. Memelink, *Methods Mol. Biol.*, 2013, **1011**, 209–225.
4 I. A. McKay, L. Kirby, E. V. Volyanik, V. Kumar, P. W. Y. Wong and S. A. Bustin, *Anal. Biochem.*, 1998, **265**, 28–34.
5 (*a*) X. Liu, L. Ouyang, X. Cai, Y. Huang, X. Feng, Q. Fan and W. Huang, *Biosens. Bioelectron.*, 2013, **41**, 218–224; (*b*) K. Peng, P. Xie, Z.-H. Yang, R. Yuan and K. Zhang, *Biosens. Bioelectron.*, 2018, **102**, 282–287.
6 (*a*) A. J. Bard and L. R. Faulkner, *Electrochem. Methods*, 2001, **2**, 482; (*b*) A. J. Bard, *Electrogenerated chemiluminescence*, CRC Press, 2004; (*c*) M. Hesari and Z. Ding, *J. Electrochem. Soc.*, 2016, **163**, H3116–H3131.
7 K. Santhanam and A. J. Bard, *J. Am. Chem. Soc.*, 1965, **87**, 139–140.
8 (*a*) G. Jie, J. Zhang, G. Jie and L. Wang, *Biosens. Bioelectron.*, 2014, **52**, 69–75; (*b*) Y. Feng, F. Sun, N. Wang, J. Lei and H. Ju, *Anal. Chem.*, 2017, **89**, 7659–7666; (*c*) J. Ye, L. Zhu, M. Yan, Q. Zhu, Q. Lu, J. Huang, H. Cui and X. Yang, *Anal. Chem.*, 2019, **91**, 1524–1531.
9 W. Y. Lee, *Microchim. Acta*, 1997, **127**, 19–39.
10 (*a*) L. Yang, Y. Zhang, R. Li, C. Lin, L. Guo, B. Qiu, Z. Lin and G. Chen, *Biosens. Bioelectron.*, 2015, **70**, 268–274; (*b*) G. Jin, C. Wang, L. Yang, X. Li, L. Guo, B. Qiu, Z. Lin and G. Chen, *Biosens. Bioelectron.*, 2015, **63**, 166–171; (*c*) Y. Lin, J. Wang, F. Luo, L. Guo, B. Qiu and Z. Lin, *Electrochim. Acta*, 2018, **283**, 798–805.
11 L. Yang, Y. Tao, G. Yue, R. Li, B. Qin, L. Guo, Z. Lin and H.-H. Yang, *Anal. Chem.*, 2016, **88**, 5097–5103.
12 (*a*) H. Wang, C. Li, X. Liu, X. Zhou and F. Wang, *Chem. Sci.*, 2018, **9**, 5842–5849; (*b*) R. M. Dirks and N. A. Pierce, *Proc. Natl. Acad. Sci. U. S. A.*, 2004, **101**, 15275–15278; (*c*) Y. Wang, J. Bai, B. Huo, S. Yuan, M. Zhang, X. Sun, Y. Peng, S. Li, J. Wang, B. Ning and Z. Gao, *Anal. Chem.*, 2018, **90**, 9936–9942.
13 X. Wang, H. Gao, H. Qi, Q. Gao and C. Zhang, *Anal. Chem.*, 2018, **90**, 3013–3018.